nature cell biology

ULK1 induces autophagy by phosphorylating Beclin-1 and activating VPS34 lipid kinase

Ryan C. Russell[1], Ye Tian[2], Haixin Yuan[1], Hyun Woo Park[1], Yu-Yun Chang[3], Joungmok Kim[1,4], Haerin Kim[1], Thomas P. Neufeld[3], Andrew Dillin[2] and Kun-Liang Guan[1,5]

Autophagy is the primary cellular catabolic program activated in response to nutrient starvation. Initiation of autophagy, particularly by amino-acid withdrawal, requires the ULK kinases. Despite its pivotal role in autophagy initiation, little is known about the mechanisms by which ULK promotes autophagy. Here we describe a molecular mechanism linking ULK to the pro-autophagic lipid kinase VPS34. Following amino-acid starvation or mTOR inhibition, the activated ULK1 phosphorylates Beclin-1 on Ser 14, thereby enhancing the activity of the ATG14L-containing VPS34 complexes. The Beclin-1 Ser 14 phosphorylation by ULK is required for full autophagic induction in mammals and this requirement is conserved in *Caenorhabditis elegans*. Our study reveals a molecular link from ULK1 to activation of the autophagy-specific VPS34 complex and autophagy induction.

Macroautophagy, hereafter referred to as autophagy, is a lysosomal-dependent cellular degradation process capable of generating nutrients and energy to maintain essential cellular activities following nutrient starvation[1]. Accumulating evidence suggests that the ULK1 protein kinase and the VPS34 lipid kinase are key regulators of autophagy initiation and progression[2–5]. Mammals have two homologues of the yeast autophagy-initiating ATG1 kinase, ULK1 and ULK2 (jointly referred to hereafter as ULK kinases)[6]. ULK1 is regulated by the nutrient- and energy-sensitive kinases TORC1 and AMPK (refs 7–11). The tight regulation of ULK activity by intracellular energy and nutrient levels is in keeping with a central role for autophagy in the protection of cells from starvation. Notably, mouse embryonic fibroblasts (MEFs) lacking FIP200, an essential component of the ULK complex, exhibit a defect in the induction of ATG14L–ATG16–WIPI puncta on starvation, indicating that ULK regulates localization of VPS34 to the phagophore[3,12]. So far, the mechanisms leading to ULK1-mediated autophagy induction remain largely undiscovered.

VPS34 is the only class III phosphoinositide 3-kinase (PI(3)K) in mammals, phosphorylating phosphatidylinositol to produce phosphatidylinositol 3-phosphate (PtdIns(3)P; ref. 13). Cellularly, PtdIns(3)P production has been implicated in promoting autophagy and retrograde trafficking from the endosomes to the Golgi[5]. The VPS34 kinase forms a stable complex with p150 (VPS15 orthologue). VPS34–p150 can also associate with Beclin-1, which serves as a binding partner for several proteins that are capable of either promoting (ATG14L, UVRAG, Bif1 and AMBRA-1) or inhibiting (Bcl2, BclxL and Rubicon) the autophagic function of VPS34 (refs 14–22). A series of studies have identified ATG14L to be essential for autophagic initiation and VPS34 activity at the phagophore[12,14,15,21,23]. Recently, AMPK was described to differentially regulate VPS34 complexes in response to glucose withdrawal[24]. However, it is not known whether or how these distinct complexes are regulated by amino-acid withdrawal, a powerful inducer of autophagy in mammalian cells.

RESULTS

ULK is required for the activation of ATG14L-associated VPS34 complexes following amino-acid withdrawal

To study the regulation of VPS34 kinase activity we performed PtdIns(3)P lipid kinase assays on complexes immunoprecipitated using antibodies against VPS34, Beclin-1 or ATG14L from cells grown in nutrient-rich or amino-acid-starved conditions. The activity of VPS34 complexes immunoprecipitated by VPS34 or Beclin-1 was reduced following starvation, whereas the activity of VPS34 complexes immunoprecipitated by ATG14L was significantly increased following amino-acid withdrawal (Fig. 1a). This is consistent with previous reports of decreased VPS34 kinase activity under amino-acid starvation using VPS34 immunoprecipitation[25–27]. ATG14L levels were low in Beclin-1 and VPS34 immunoprecipitates, explaining the starvation-induced decrease in VPS34 activity in these complexes despite their ability to bind ATG14L (Fig. 1a,b). These data indicate

[1]Department of Pharmacology and Moores Cancer Center, University of California San Diego, La Jolla, California 92093, USA. [2]Department of Molecular and Cell Biology, University of California Berkeley, Berkeley, California 94720, USA. [3]Department of Genetics, Cell Biology and Development, University of Minnesota, Minneapolis, Minnesota 55455, USA. [4]Department of Oral Biochemistry, School of Dentistry, Kyung Hee University, Seoul 130-701, Korea.
[5]Correspondence should be addressed to K-L.G. (e-mail: kuguan@ucsd.edu)

Received 6 June 2012; accepted 15 April 2013; published online 19 May 2013; DOI: 10.1038/ncb2757

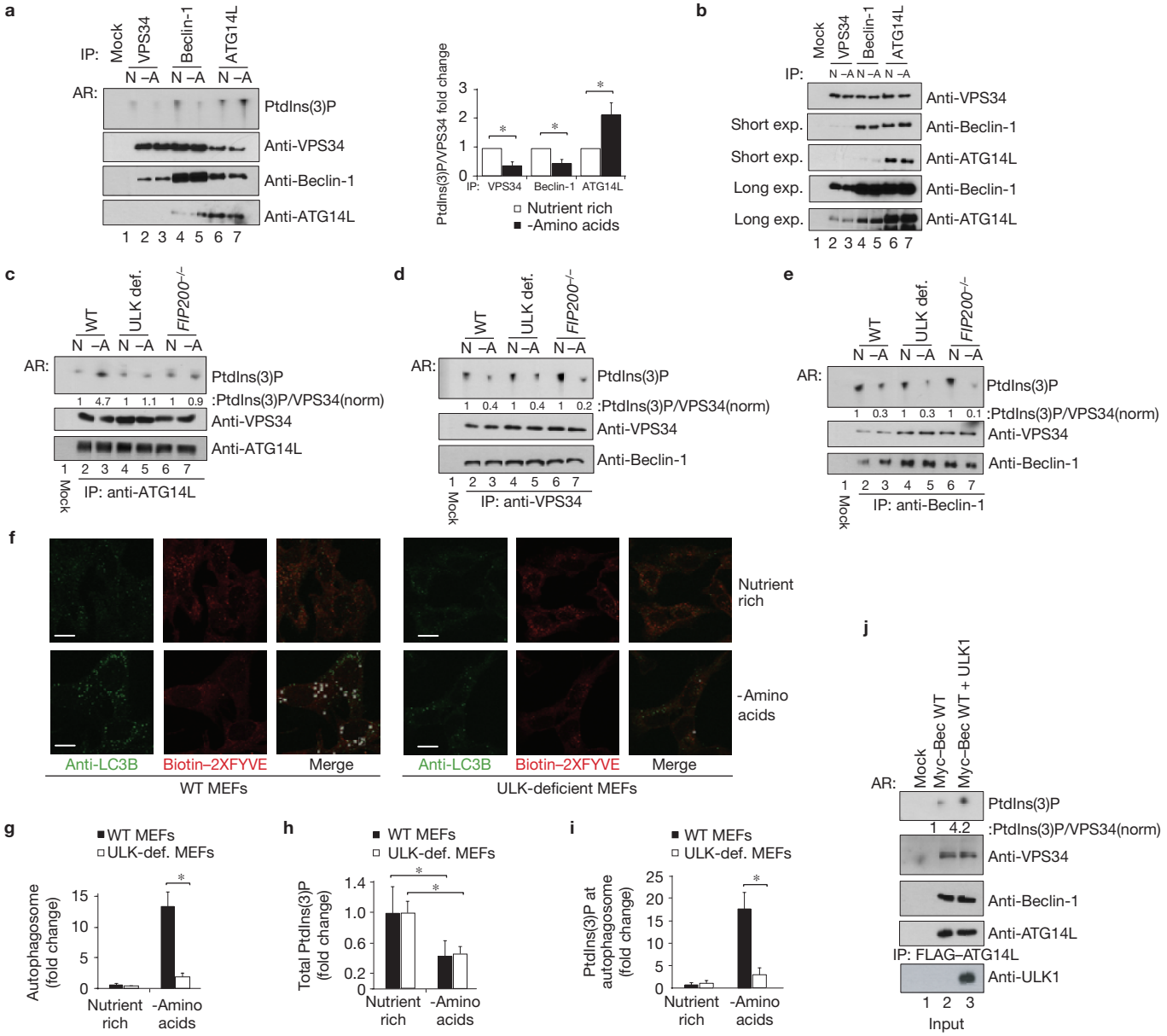

Figure 1 ULK is essential for activation of the ATG14L-associated VPS34 following amino-acid starvation. Unless otherwise stated, experiments were repeated three times; data shown are representative. (**a**) Different VPS34 complexes were immunoprecipitated (IP) from MEFs in the presence (N) or absence (−A) of amino acids using the indicated antibodies and assayed for kinase activity (left, top panel). Inputs were immunoblotted using the antibodies indicated (left, lower panels). Quantification of VPS34 activity is from 3 biological repeats (right panel; data shown are mean + s.d.). AR, autoradiography. (**b**) Immunoprecipitation of three VPS34 complexes, normalized for VPS34, was performed using the indicated antibodies under nutrient-rich (N) or starvation (-A) conditions. VPS34-binding partners were analysed by western blotting. (**c**) ATG14L-containing VPS34 complexes were immunopurified from WT, *ULK1*$^{-/-}$ 2KD (ULK def.) and *FIP200*$^{-/-}$ MEFs, and measured for lipid kinase activity as in **a**. (**d**) VPS34 was immunopurified from WT, ULK-deficient and *FIP200*$^{-/-}$ MEFs. A kinase assay was performed as in **a**. (**e**) Immunoprecipitation of Beclin-1-containing VPS34 complexes from WT, ULK-deficient and *FIP200*$^{-/-}$ MEFs. A kinase assay was performed as in **a**. (**f**) LC3B puncta and PtdIns(3)P levels were analysed with anti-LC3B and the biotin–2XFYVE domain probe. Representative immunofluorescence images of LC3B and 2XFYVE domain binding are shown (scale bars, 10 μm). (**g**) Quantification of LC3B puncta from **f**. Details of quantification are provided in the Methods; Data shown in **g**–**i** are mean + s.d. from a minimum of 6 unique fields of view from a representative experiment (see statistical source data in Supplementary Table S1). (**h**) Total PtdIns(3)P was quantified from the experiment in **f**. Error bars were calculated as in **g**. (**i**) Quantification of PtdIns(3)P that co-localizes with LC3B on amino-acid withdrawal from the experiment described in **f**. (**j**) VPS34 activity with or without ULK1 overexpression was assayed. A representative experiment of four repeats is shown. $^{*}P < 0.05$ (**a**,**g**,**h**,**i**) as determined by Student's *t*-test (see statistical source data in Supplementary Table S1 and Methods). Quantification of PtdIns(3)P/VPS34 provided under the PtdIns(3)P panel in **c**–**e**,**j** nutrient-rich conditions was normalized to 1. Uncropped images of blots are shown in Supplementary Fig. S4.

that a differential regulation of VPS34 complexes exists in response to amino-acid starvation. It has been reported that the autophagy-specific function of VPS34 can be regulated by the disruption of the VPS34 kinase complex, under extended starvation. Starvation with Hanks' balanced salt solution for several hours results in a phosphorylation of the non-structured loop of Bcl-2 and dissociation

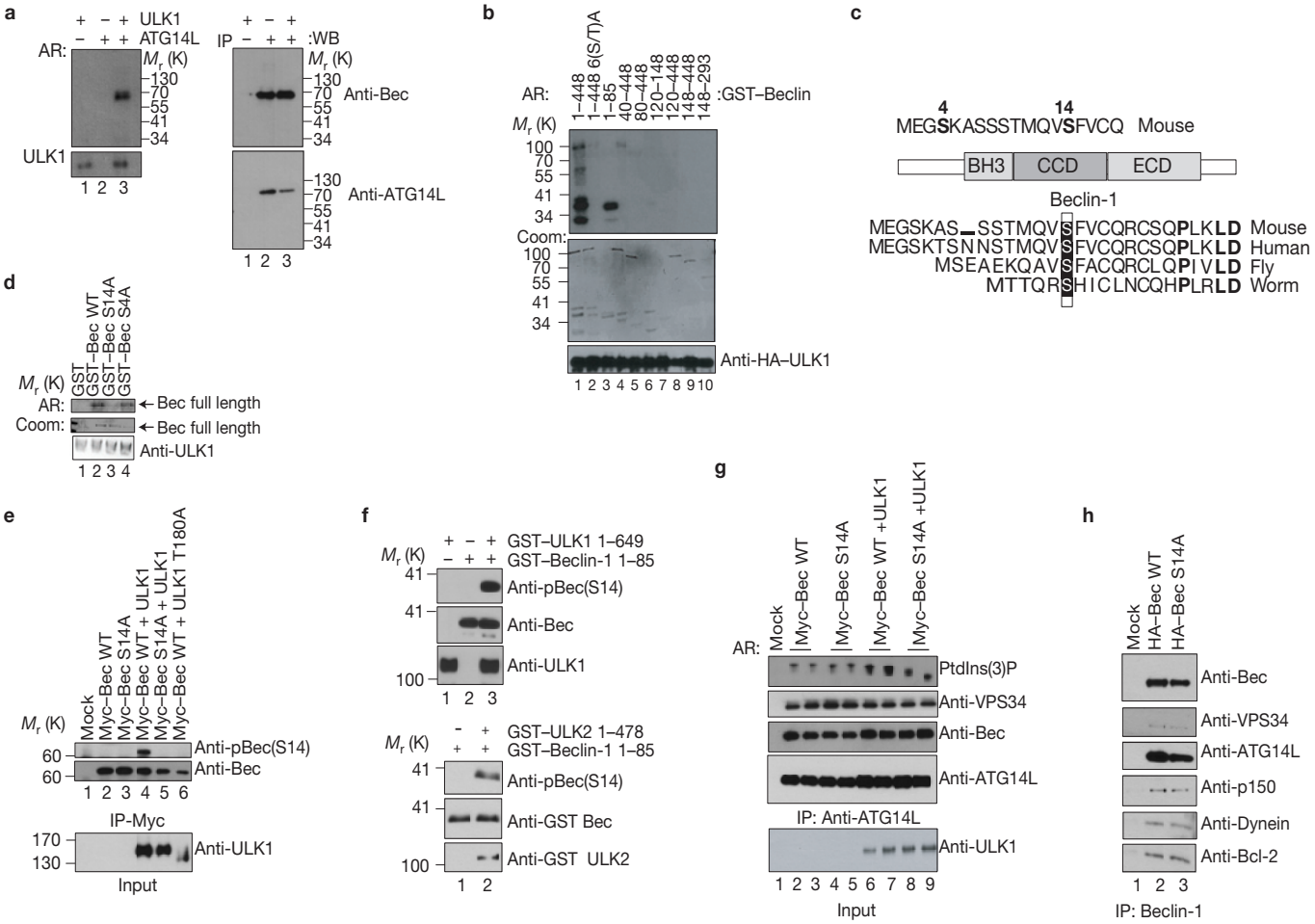

Figure 2 Beclin-1 Ser 14 is phosphorylated by ULK1 and required for VPS34 activation in response to amino-acid withdrawal. Unless otherwise stated, all experiments were repeated three times and the data shown are representative. (**a**) HEK293 cells were transfected with ATG14L, VPS34 and Beclin-1. ATG14L-containing VPS34 complexes were immunopurified and subjected to an *in vitro* ULK1 kinase assay in the presence of γ-^{32}P[ATP]. Bound ATG14L complexes and soluble ULK1 were separated and phosphorylation was detected by autoradiography (AR, left panels). Western blotting was performed (right panels). Results are representative of two unique experiments. (**b**) Full-length murine GST–Beclin-1 and various truncations (as labelled) were subjected to an *in vitro* HA–ULK1 kinase assay. GST–Beclin-1 6(S/T)A has serine/threonine residues 4, 7, 10, 14, 29 and 42 mutated to alanine. ULK1 inputs were determined by western blotting, Beclin-1 inputs by Coomassie (Coom) and target phosphorylation by autoradiography. (**c**) GST–Beclin-1 (1–85) was subjected to an *in vitro* ULK1 kinase reaction and analysed by mass spectrometry. Ser 14, Ser 15 in humans (outlined), is the main phosphorylation site identified (for mass spectrometry data, see Supplementary Fig. S2b,c). Mass spectrometry was performed on a single experiment. (**d**) Beclin-1 Ser 14 is the main *in vitro* ULK1 phosphorylation site. Beclin-1 WT, and S4A and S14A mutants were subjected to an *in vitro* ULK1 kinase assay. The reaction was developed by autoradiography and stained for Beclin-1 input levels by Coomassie blue. Results are representative of two unique experiments. (**e**) HEK293 cells were transfected with the indicated plasmids under nutrient-rich conditions. Beclin-1 was immunoprecipitated and immunoblotted with pBeclin-1(Ser 14), or anti-Beclin-1 as a loading control. ULK1 inputs are included below immunoprecipitated samples. (**f**) Purified GST–Beclin-1 (1–85) was subjected to *in vitro* phosphorylation by GST–ULK1 (top panel) and GST–ULK2 (bottom panel). Reactions were immunoblotted with the indicated antibodies. (**g**) HEK293 cells were transfected with ATG14L, VPS34 and Beclin-1 and grown under nutrient-rich conditions. ATG14L-containing VPS34 complexes were immunoprecipitated and lipid kinase activity was assayed as described in Fig. 1j. Inputs were immunoblotted with the indicated antibodies. Representative of four unique experiments. (**h**) Stable lines containing Beclin-1(WT or S14A) were used for Beclin-1 immunoprecipitation. Binding partners were determined by SDS–PAGE analysis and western blot using the indicated antibodies. Uncropped images of blots are shown in Supplementary Fig. S4.

from Beclin-1 (ref. 28). Under the starvation conditions used in this study we observed no significant change in Beclin-1–VPS34 interaction, consistent with previous observations[25]. The activation of ATG14L-containing VPS34 complexes provides a description of a unique mode of VPS34 regulation that does not necessitate the destabilization of the VPS34–Beclin-1 interaction.

To determine the requirement for ULK kinase in this activation we performed lipid kinase assays in wild-type (WT) MEFs or two MEF lines deficient for ULK activity. Both ULK1-knockout MEFs with ULK2 stable knockdown (ULK-deficient MEFs, described previously[10]) and FIP200-knockout MEFs are defective for ULK activity. FIP200 is an essential cofactor for both ULK1&2, which perform redundant roles in autophagy[3,29]. Interestingly, ATG14L-containing VPS34 complexes were not activated on starvation in both ULK-deficient cell lines (Fig. 1c). However, the starvation-induced repression of VPS34 complexes purified by VPS34 (Fig. 1d) or Beclin-1 (Fig. 1e)

antibody was retained in FIP200-null and ULK-deficient MEFs. Therefore, ULK kinase is required only for the activation of the pro-autophagic ATG14L-containing VPS34 complex and not the repression of non-autophagic VPS34 complexes. The inability of ATG14L-containing VPS34 complexes to be activated was accompanied by a reduction in autophagy induction in ULK- and FIP200-deficient cells (Supplementary Fig. S1a) as well as a reduction of endogenous LC3B puncta (Supplementary Fig. S1b,c).

To measure PtdIns(3)P at the autophagosome we performed co-staining for endogenous LC3B and PtdIns(3)P using an anti-LC3B antibody and a biotinylated 2XFYVE domain probe, respectively. Biotin–2XFYVE specifically binds PtdIns(3)P through its two FYVE domains and has been used previously to monitor PtdIns(3)P on endosomes when co-stained with an endosomal marker[30]. Under starvation the total number of PtdIns(3)P puncta decreased in WT cells (Fig. 1f,h). Conversely, the number of PtdIns(3)P puncta co-localizing to autophagosomes, as marked by the LC3B staining, increased (Fig. 1f,i). Similarly to WT MEFs, ULK-deficient cells showed a decrease in total PtdIns(3)P puncta under starvation conditions (Fig. 1f,h). In contrast, ULK-deficient cells showed a clear defect in the induction of PtdIns(3)P-positive autophagosomes under starvation conditions (Fig. 1f,i). The defect of ULK-deficient MEFs in LC3B puncta accumulation and PtdIns(3)P–LC3B double-positive puncta on starvation were similarly observed in *FIP200*$^{-/-}$ MEFs (Supplementary Fig. S1b,c,e), which retained the ability to repress total PtdIns(3)P (Supplementary Fig. S1b,d). Importantly, pharmacological inhibition of VPS34 completely abolished both 2XFYVE probe labelling and LC3B puncta induced by amino acid starvation, showing the specificity of these staining techniques (Supplementary Fig. S1f). Together, these data support a critical role for ULK in regulating the autophagy-specific ATG14L-containing VPS34 complex activity.

To determine whether ULK1 is sufficient to activate ATG14L-containing VPS34 complexes, ATG14L was immunoprecipitated from HEK293 cells cotransfected with myc–Beclin-1, Flag–ATG14, HA–VPS34 and empty vector or HA–ULK1 under nutrient-rich conditions. Activity of the ATG14L-containing VPS34 complexes was markedly increased on ectopic expression of ULK1, indicating that ULK1 activates the ATG14L-containing VPS34 complexes (Fig. 1j). These results demonstrate that distinct VPS34 kinase complexes are differentially regulated in response to nutrient starvation and ULK activity is critical for activation of ATG14L-containing VPS34 complexes in response to amino-acid starvation.

Beclin-1 phosphorylation by ULK1 is required for activation of ATG14L-bound VPS34 in response to amino-acid starvation

We sought to determine whether ULK1 could directly phosphorylate any member of the VPS34 complex. ATG14L-containing VPS34 complexes were immunopurified from transfected cells and subjected to an *in vitro* ULK1 kinase assay using [γ-^{32}P]ATP. Autoradiography showed a single predominant band with a relative molecular mass of approximately 60,000 (M_r 60K; Fig. 2a, left panel). Western blotting confirmed co-migration of the autoradiography band with Beclin-1 but not ATG14L (Fig. 2a). To map the phosphorylation site on Beclin-1 we performed ULK1 *in vitro* kinase assays with [γ-^{32}P]ATP on various Beclin-1 deletions. ULK1 was capable of phosphorylating

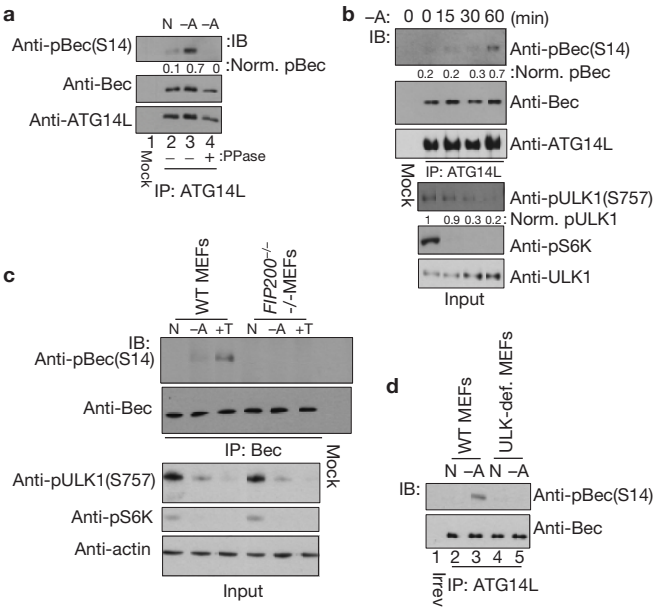

Figure 3 Beclin-1 is a physiological target of ULK kinase in response to amino-acid withdrawal and mTOR inhibition. Unless otherwise stated, all experiments were repeated three times and data shown are representative. (**a**) WT MEFs were cultured with or without amino acids. ATG14L-associated Beclin-1 was immunoprecipitated and treated with lambda phosphatase treatment (PPase) as indicated. Western blotting (immunoblotting, IB) was performed with the indicated antibodies. Beclin-1 Ser 14 phosphorylation was quantified (shown under top panel) and normalized to total Beclin-1. (**b**) WT MEFs were starved for the indicated times. Beclin-1 was immunopurified by ATG14L immunoprecipitation and immunoblotted as indicated (top panels). Whole-cell lysates were immunoblotted with pULK1 S757 (mTORC1-target site), pS6K and ULK1 antibodies (bottom panels). Two unique experiments were performed. (**c**) WT or *FIP200*$^{-/-}$ MEFs were incubated under nutrient-rich, amino-acid-deprived or Torin-1 (+T, an mTOR inhibitor) conditions. Beclin-1 was purified and immunoblotted as in Fig. 3b. (**d**) WT or ULK-deficient MEFs were incubated with or without amino acids. Beclin-1 was purified and immunoblotted as in **a**. Two unique experiments were performed. Uncropped images of blots are shown in Supplementary Fig. S4.

all truncations that shared the amino-terminal 85 amino acids (Supplementary Fig. S2a).

We next sought to identify putative ULK1 phosphorylation sites in the N terminus of Beclin-1 by mutagenesis and truncations. Deletion of the N-terminal 40 amino acids largely abolished ULK1-mediated phosphorylation (Fig. 2b). Conserved serine and threonine residues in the N terminus of mouse Beclin-1 were mutated to alanine (S/T(4,7,10,14,29,42)A). The Beclin-1 S/T(4,7,10,14,29,42)A mutant was not phosphorylated by ULK1 (Fig. 2b, lane 2), indicating that one or more of the six residues are ULK1 phosphorylation sites. In conjunction we performed mass spectrometry analysis on an N-terminal fragment of Beclin-1 after performing an *in vitro* ULK1 kinase reaction. Two phosphorylation sites were detected (Fig. 2c and Supplementary Fig. S2b,c), one with low confidence, Ser 4, and one with high confidence, Ser 14, which is conserved to *C. elegans* (Fig. 2c, bottom).

The peptide encompassing conserved Ser 63 was not detected by mass spectrometry, so the GST–Beclin-1 1–85 S/T(4,7,10,14,29,42,63)A mutant was made. In this background Ala 4 and 14 were singly

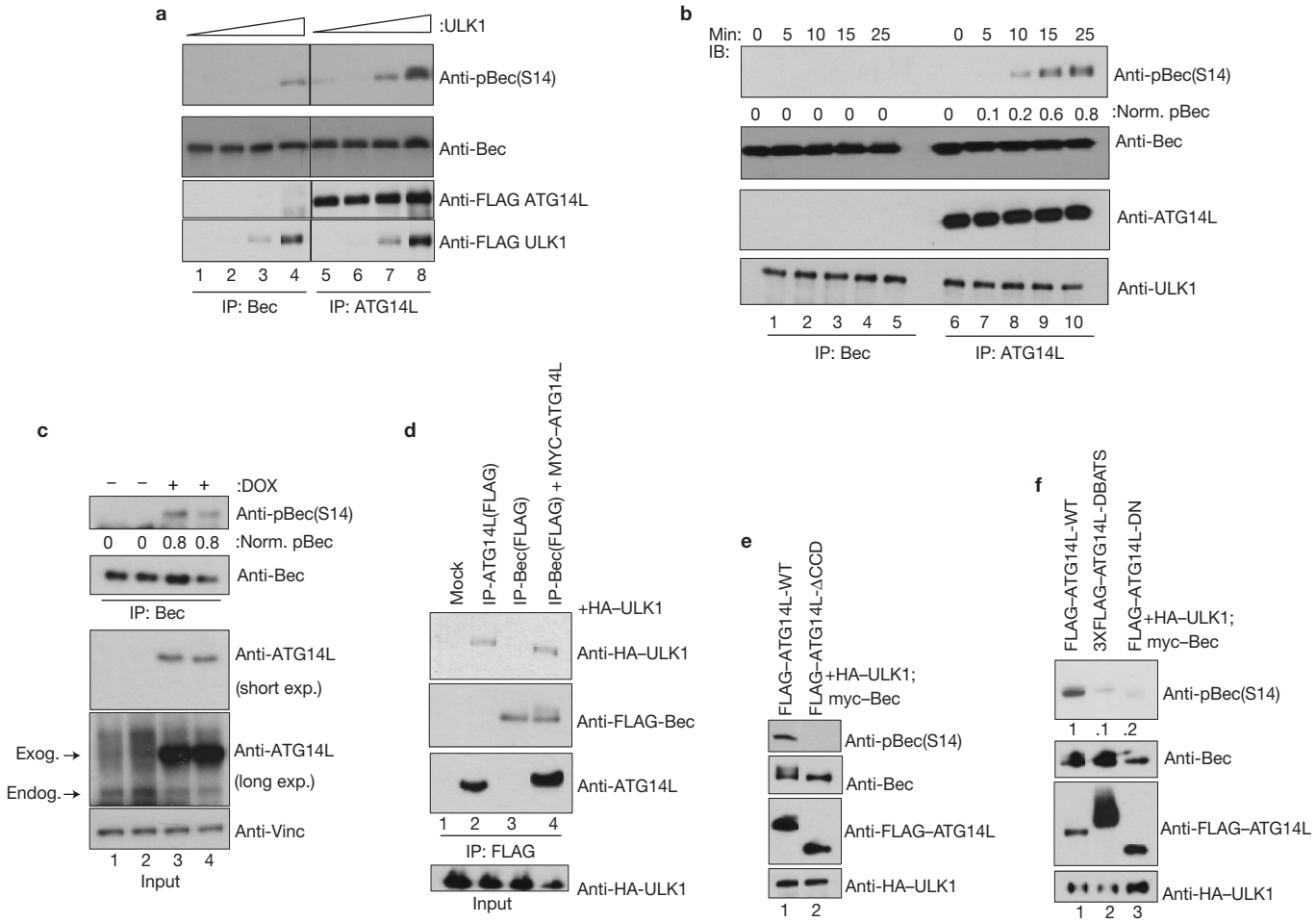

Figure 4 ATG14L stimulates Beclin-1 Ser 14 phosphorylation by promoting association with ULK1. Unless otherwise stated all experiments were repeated three times and data shown are representative. (**a**) Beclin-1 alone (lanes 1–4) or Beclin-1 and ATG14L (lanes 5–8) were overexpressed in HEK293 cells. Beclin-1 was purified either by direct immunoprecipitation (lanes 1–4) or by ATG14L immunoprecipitation (lanes 5–8). Immunoprecipitated samples were subjected to an *in vitro* ULK1 kinase assay with increasing amounts of ULK1. Reactions were immunoblotted with the indicated antibodies. Black line denotes discontinuous lanes from the same gel. Two unique experiments were performed. (**b**) Beclin-1 alone or bound to ATG14L was purified as described in **a**. Equal amounts of ULK1 were added to each complex and reactions were quenched at the indicated time points. Western blotting was performed with the indicated antibodies. (**c**) An ATG14L–FLAG-6His-inducible U2OS cell line was induced for 16 h in the presence of amino acids. Endogenous Beclin-1 was immunoprecipitated and immunoblotted as in Fig. 3a. ATG14L input levels were detected by immunoblotting. Two unique experiments were performed. (**d**) HEK293 cells transfected with either ATG14L or Beclin-1, or both, in conjunction with ULK1, were immunoprecipitated as indicated and blotted with the indicated antibodies. (**e**) HEK293 cells were transfected with Beclin-1 and ULK1 in the presence of ATG14L WT or ATG14LΔCCD, which is defective in Beclin-1 binding, under nutrient-rich conditions. Lysates were resolved by SDS–PAGE and blotted with the indicated antibodies. (**f**) HEK293 cells were transfected with ULK1 and Beclin-1 in conjunction with either ATG14L WT, or one of two mutants (ΔBATS, ΔN) that are defective in phagophore localization. Samples were handled as in **e**. Uncropped images of blots are shown in Supplementary Fig. S4.

mutated back to serine. Recovery of Ser 14 restored ULK-mediated phosphorylation, whereas recovery of Ser 4 had no effect (Supplementary Fig. S2d). To confirm the main phosphorylation site for ULK1, Ser 4 and 14 were singly mutated to alanine in mouse Beclin-1. Mutation of Ser 14 abolished ULK1-mediated phosphorylation whereas mutation of Ser 4 had no effect, indicating that Ser 14 (corresponding to Ser 15 in human) is the primary ULK1 phosphorylation site in Beclin-1 (Fig. 2c,d).

To determine whether ULK1 phosphorylates Beclin-1 Ser 14 *in vivo* we generated a phospho-specific antibody. To test the specificity of the antibody, cells were transfected with Beclin-1(WT or S14A) with or without ULK1 (WT or kinase inactive). Co-expression of the WT ULK1, but not a catalytically inactive mutant, induced Beclin-1 Ser 14 phosphorylation (Fig. 2e)[31]. As expected no phosphorylation was observed in Beclin-1 S14A (Fig. 2e, lane 5). These data indicate that ULK1 can phosphorylate Beclin-1 in cells and validate the specificity of the phospho-antibody. To exclude the possibility that an ULK-associated kinase was responsible for Beclin-1 phosphorylation, we used ULK1 purified from insect cells for an *in vitro* kinase assay using recombinant Beclin-1 from *Escherichia coli*. Immunoblotting of the resulting kinase reaction showed robust Beclin-1 phosphorylation, indicating that Beclin-1 is a direct target of ULK1 (Fig. 2f and Supplementary Fig. S2e). We investigated whether ULK2 is similarly capable of phosphorylating Beclin-1. ULK2 kinase purified from insect cells also phosphorylated Beclin-1 at Ser 14, indicating a redundancy for the ULK kinases in promoting Beclin-1 phosphorylation (Fig. 2f, bottom panel).

We next sought to determine whether Beclin-1(Ser 14) phosphorylation was required for ULK1-mediated activation of the ATG14L-associated VPS34 lipid kinase. ATG14L was immunoprecipitated from transfected cells and an *in vitro* PtdIns(3)P lipid kinase assay was performed. As previously shown, ULK1 cotransfection enhanced VPS34 kinase activity (Fig. 2g, compare lanes 2&3 with 6&7); however, ATG14L VPS34 complexes containing mutant Beclin-1 did not respond to ULK1 cotransfection (Fig. 2g, compare lanes 4&5 with 8&9). Importantly, we found that abrogation of the ULK1 phosphorylation site in Beclin-1 had no discernible effect on its ability to bind VPS34, ATG14L, p150, dynein and Bcl2 (Fig. 2h). These data indicate that direct phosphorylation of Beclin-1 on Ser 14 by ULK1 is required for activation of the autophagy-specific VPS34 kinase complex.

Ser 14 of Beclin-1 is phosphorylated by ULK kinase in response to amino-acid withdrawal and mTOR inhibition

To determine whether Beclin-1 is a physiological target of ULK1, ATG14L-associated Beclin-1 was immunopurified from WT MEFs. Western blot analysis showed that endogenous Beclin-1 is phosphorylated following amino-acid starvation, and phosphatase treatment completely abolished the Beclin-1 phospho-Ser 14 signal (Fig. 3a). ULK1 activity is potently repressed by TORC1 phosphorylation. To determine whether there is a correlation between Beclin-1(Ser 14) phosphorylation and TORC1 signalling to ULK1, an amino-acid withdrawal time course was performed. As expected, phosphorylation of ULK1 (Ser 757, the TORC1 target site) decreased on amino-acid withdrawal, although more slowly than the dephosphorylation of S6K (another TORC1 substrate) (Fig. 3b). Interestingly, ULK1-mediated Beclin-1 phosphorylation inversely correlated with the inhibitory phosphorylation on ULK1 (Fig. 3b). To determine whether inhibition of TORC1 was sufficient to activate ULK1-mediated Beclin-1 phosphorylation, WT or *FIP200*$^{-/-}$ and ULK-deficient MEFs were treated with mTOR catalytic inhibitor, Torin-1, under nutrient-rich conditions or with amino-acid withdrawal. Inhibition of mTOR resulted in a clear induction of Beclin-1 Ser 14 phosphorylation only in the WT MEFs, indicating that relief of mTOR-mediated inhibition of ULK1 stimulates downstream target phosphorylation (Fig. 3c,d).

ATG14L promotes Beclin-1 phosphorylation by enhancing association with ULK1

The regulation of VPS34 lipid kinase activity by ULK1 is limited to the ATG14L-containing complex (Fig. 1c); therefore, we investigated whether ULK1 would exhibit a preference for phosphorylation of the ATG14L-bound Beclin-1. Beclin-1 alone or ATG14L-bound Beclin-1 was immunoprecipitated from transfected cells. Endogenous ATG14L co-precipitated from cells overexpressing Beclin-1 alone was negligible compared with the levels from complexes obtained from cells transfected with both Beclin-1 and ATG14L (Fig. 4b). Both complexes were used as substrates for ULK1 *in vitro* kinase assays. We found that ATG14L-containing Beclin-1 was efficiently phosphorylated by ULK1 whereas Beclin-1 alone was a comparatively poor substrate (Fig. 4a,b), indicating that ATG14L makes Beclin-1 a better substrate for ULK1 (Fig. 4b). To determine whether ATG14L plays a role in promotion of Beclin-1 phosphorylation *in vivo* we used an ATG14L-inducible cell line. Induction of ATG14L overexpression promoted Beclin-1

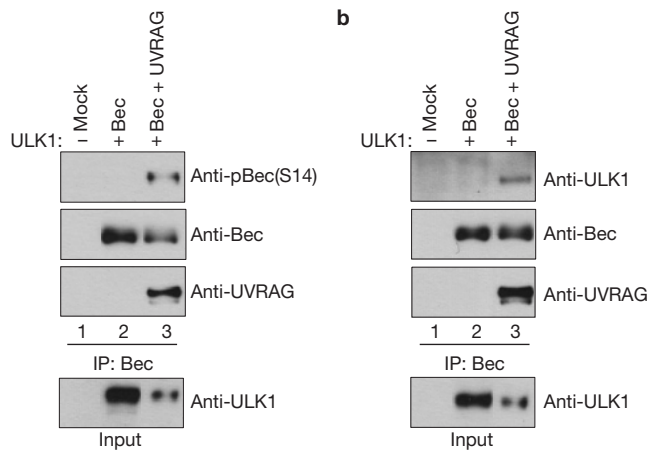

Figure 5 UVRAG promotes Beclin-1 Ser 14 phosphorylation and association with ULK1. (**a**) HEK293 cells were transfected with Beclin-1, with or without UVRAG, in conjunction with ULK1 as indicated in the presence of amino acids. Lysates were immunoblotted with the indicated antibodies. A representative experiment of three repeats is shown. (**b**) UVRAG bridges the interaction between Beclin-1 and ULK1. HEK293 cells were transfected with Beclin-1, with or without UVRAG, in conjunction with ULK1 as indicated. Lysates were immunoprecipitated with anti-HA(Beclin-1) antibody and blotted with the indicated antibodies. A representative experiment of three repeats is shown. Uncropped images of blots are shown in Supplementary Fig. S4.

phosphorylation (Fig. 4c), further supporting that ATG14L-bound Beclin-1 is the preferred target of ULK1 *in vivo*.

To understand the mechanism underlying the ATG14L-mediated promotion of Beclin-1 phosphorylation we performed immunoprecipitation assays to determine the interaction of ATG14L and Beclin-1 with ULK1 when expressed alone or together. Interestingly, we found that immunoprecipitation of Beclin-1 pulled down ULK1 only when co-transfected with ATG14L (Fig. 4d, compare lanes 3 and 4). Conversely, immunoprecipitation of ATG14L could pull down ULK1 in the absence of Beclin-1, suggesting that ATG14L may recruit Beclin-1 to ULK1 for phosphorylation (Fig. 4d, lane 2). To confirm that ATG14L stimulates Beclin-1 phosphorylation by promoting an ULK1–ATG14L–Beclin-1 complex, we cotransfected ATG14L WT or ATG14L ΔCCD (a mutant deficient in Beclin-1 binding) with Beclin-1 and ULK1 (refs 14,15). We found that the ability of ATG14 to stimulate Beclin-1 phosphorylation was completely lost in ATG14LΔCCD (Fig. 4e). The mechanistic model where ATG14L acts as an adaptor to recruit ULK1 to Beclin-1 is further supported by the fact that promotion of Beclin-1 phosphorylation is preserved in the *in vitro* kinase reaction (Fig. 4b).

Recruitment of ATG14L-containing VPS34 complexes to the phagophore requires ULK1. Therefore, we examined whether localization of ATG14L to the phagophore took place upstream or downstream of Beclin-1 Ser 14 phosphorylation. We found that removal of the BATS (Barkor/Atg14L autophagosome targeting sequence) domain or extreme N-terminus of ATG14L, both of which are necessary for the localization of ATG14L to the phagophore[23,32], but not binding to Beclin-1, severely compromised Beclin-1 phosphorylation when compared with WT control (Fig. 4f). Previously, phosphorylation of AMBRA-1 by ULK1 was shown to be required for localization of Beclin-1 to the phagophore[18], making the activation of the ATG14L-containing VPS34 kinase a downstream

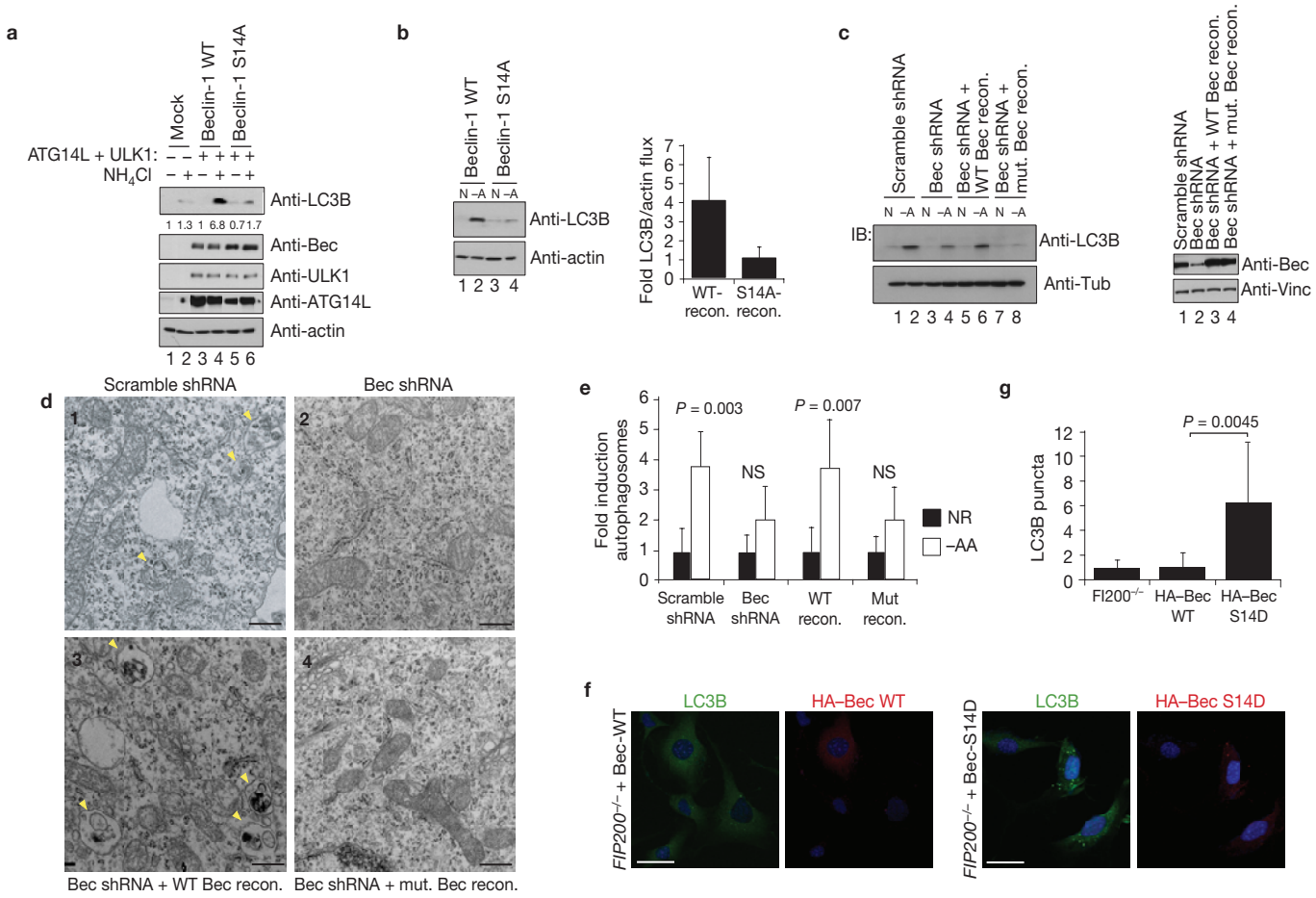

Figure 6 Beclin-1 Ser 14 phosphorylation plays a critical role in autophagy induction by amino-acid starvation. Unless otherwise stated, all experiments were repeated three times and data shown are representative. (**a**) HEK293 cells were transfected with the indicated plasmids. Cells were grown in the presence of amino acids and treated with NH_4Cl to block autophagic turnover where indicated. Lysates were immunoblotted with the indicated antibodies. (**b**) HEK293 cells transfected with Beclin-1 ATG14L were grown in the presence or absence of amino acids. Lysates were immunoblotted with the indicated antibodies (left panel) and quantified by densitometry (right panel). Data represent mean + s.d. of three unique experiments. (**c**) Beclin-1-shRNA reconstituted lines (WT or mutant) and controls (scramble shRNA or Beclin-1 shRNA) were grown with or without amino acids and assessed for autophagy (left panel) and Beclin-1 levels (right panel). (**d**) Autophagosome (denoted by arrowheads) generation on amino-acid withdrawal was analysed by electron microscopy. Cell lines and conditions from **c** were used and representative images from the indicated amino-acid-starved lines are shown; scale bars, 0.4 μm. (**e**) Quantification of **d**. Fold induction was determined by arbitrarily making the nutrient-rich condition 1 (solid bars) for each line. Error bars represent the s.d. of the mean value over an average of 20 fields of view within a representative experiment. NS, not significant. (**f**) HA–Beclin-1 WT or S14D was transiently expressed in *FIP200*$^{-/-}$ MEFs grown under nutrient-rich conditions. Indirect immunofluorescence was performed using antibodies against endogenous LC3B and HA–Beclin-1. Scale bars, 20 μm. (**g**) Quantification of LC3B puncta from confocal in **f**. In the HA–Beclin-1- or HA–Beclin-1-S14D-transfected samples, only the HA-positive cells were counted for LC3B puncta. Error bars were processed as in **e**. Mean value shown; *P* values determined by Student's *t*-test using 10 unique fields of view from **f**. Uncropped images of blots are shown in Supplementary Fig. S4.

event. Furthermore, the reported role for ULK1 in the regulation of ATG9 cycling from the *trans*-Golgi network to endosomes can be blocked by inhibition of VPS34, putting ATG9 regulation downstream of ULK-mediated activation of ATG14L–VPS34 complexes[2].

This complex and multifaceted regulation of VPS34 kinase by ULK probably underscores the pivotal role for autophagy induction in the cellular response to starvation.

UVRAG promotes phosphorylation of Beclin-1 by ULK1

Beclin-1 also binds ultraviolet radiation resistance-associated gene protein (UVRAG) to promote the maturation of the autophagosome and this complex is known to be free of ATG14L. Therefore, we examined whether UVRAG plays a similar role in promoting Beclin-1 phosphorylation as ATG14L. Indeed, UVRAG bound Beclin-1 preferentially associated with ULK1 and overexpression of UVRAG promoted Beclin-1 phosphorylation (Fig. 5a,b). UVRAG binds only a small minority of the total Beclin-1 and represents a minor fraction of total Beclin-1-associated VPS34 activity[24]. Therefore, in addition to regulating autophagy initiation through ATG14L complexes it is possible that Beclin-1 phosphorylation may also play a role in the autophagosome maturation through regulation of the UVRAG-containing VPS34 complex.

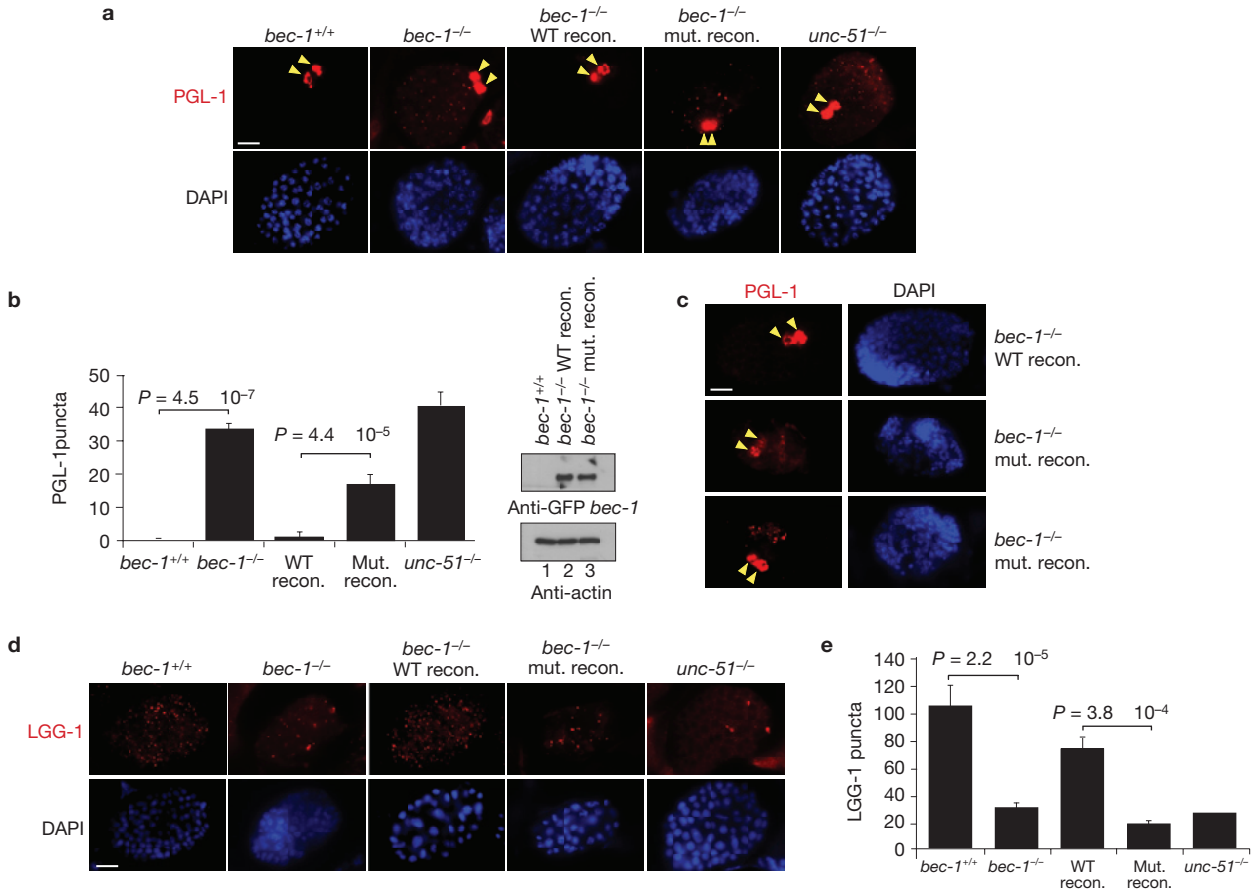

Figure 7 The conserved ULK phosphorylation site in *C. elegans Bec-1* is required for autophagy. Unless otherwise stated, all experiments were repeated three times and data shown are representative. (**a**) *Bec-1 C. elegans* were reconstituted with either WT or mutant GFP–BEC-1. Stable worm lines with *Bec-1* rescue were obtained and embryos were stained with anti- PGL-1 antibody. Arrowheads indicate normal PGL-1 staining in germline cells. (**b**) Quantification of PGL-1 puncta outside germline cells (left panel). Error bars represents s.d. between 3 unique embryos in a representative experiment. Reconstituted *Bec-1* (WT and mutant) levels in *Bec*$^{-/-}$ stable worms were compared by western blotting. Mean value presented. (**c**) Spectrum of defects in PGL granule degradation in *bec-1* mutant rescue embryos. Mutant embryos exhibited either high levels of diffuse PGL-1 staining (middle-left panel; one-third of the embryos), or large punctuate PGL-1 structures in somatic cells (bottom-left panel; two-thirds of the embryos). Both diffuse or punctuate PGL-1 staining in somatic cells have been described in autophagy-deficient embryos. (**d**) Embryos from the lines described in **a** were labelled with anti-LGG-1, along with WT and *unc*-51 worms. Representative embryos at ~100 cell stage are shown. (**e**) Quantification of LGG-1 per embryo from labelling in **d**. Error bars generated as in **b**. Mean value presented. Uncropped images of blots are shown in Supplementary Fig. S4. Scale bar, 10 μm.

Phosphorylation of Beclin-1 is required for induction of autophagy in response to amino-acid starvation

We previously showed that ATG14L-associated VPS34 complexes containing Beclin-1 S14A could not be activated by ULK1 (Fig. 2g). We investigated whether this lack of activation results in an overall deficiency in autophagy. Cotransfection of ULK1 with WT Beclin-1 and ATG14L strongly increased autophagic flux as indicated by the increase of LC3B II accumulation (Fig. 6a). Comparatively, cotransfection of phospho-defective Beclin-1 S14A attenuated ULK-mediated activation of autophagic flux (Fig. 6b), indicating that activation of the ATG14L-containing VPS34 complex may be required for autophagy induction.

To further elucidate the role of ULK1–Beclin-1-Ser-14 phosphorylation in the promotion of autophagy we generated knockdown-reconstitution stable cell lines (see Methods). Cell lines expressing a scrambled non-targeting short hairpin RNA (shRNA) or Beclin-1 shRNA without reconstitution served as controls. Reconstituted Beclin-1 levels were comparable to that of endogenous Beclin-1 (Fig. 6c). The WT and mutant Beclin-1 showed similar localization (Supplementary Fig. S3c). Starvation of cells containing Beclin-1 knockdown or with mutant Beclin-1 reconstitution showed a reduction in LC3B II accumulation when compared with scramble shRNA or WT Beclin-1 reconstituted control (Fig. 6c). To validate these findings we performed a similar experiment and analysed the cells by electron microscopy. Consistent with previous observations we found that Beclin-S14A and Beclin-1-shRNA lines did not produce a significant increase in autophagosomes on amino-acid starvation (Fig. 6d,e). Conversely, scramble shRNA and WT-Beclin-1 reconstituted lines showed a significant accumulation of autophagosomes when starved for amino acids (Fig. 6d,e). The lack of autophagosome induction in mutant Beclin-1 reconstituted HeLa cells was also determined quantitatively by scoring of LC3B puncta accumulation (Supplementary Fig. S3a,b). These data indicate that phosphorylation of Beclin-1 by ULK kinase is required for an appropriate autophagic response on amino-acid withdrawal.

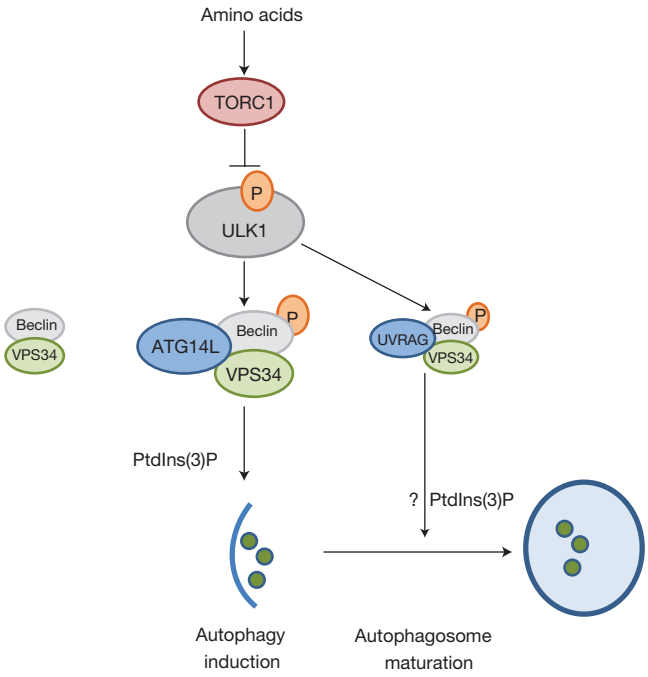

Figure 8 A working model of VPS34 complex regulation by ULK on amino-acid withdrawal. Amino-acid starvation inactivates TORC1, de-repressing ULK1. ULK1 is recruited to VPS34–Beclin-1 complexes through binding to ATG14L, phosphorylating Beclin-1, and activating the VPS34 kinase and PtdIns(3)P production at the nascent autophagosome. In addition, UVRAG-bound Beclin-1 is phosphorylated by ULK1, which may promote autophagosome maturation.

We next sought to determine whether autophagy could be driven by introduction of a phospho-mimetic residue at Ser 14 of Beclin-1. HA–Beclin-1(WT and S14D) were transiently expressed in the *FIP200*$^{-/-}$ background. Induction of autophagy was determined by quantification of LC3B puncta in Beclin-1- expressing cells versus their non-expressing neighbours. Overexpression of WT Beclin-1 had no significant effect on inducing LC3B puncta (Fig. 6f, top panels). However, most cells expressing Beclin-1 S14D had significantly more LC3B puncta than the *FIP200*$^{-/-}$ background (Fig. 6f, bottom panels). The induction of autophagy by the Beclin-1 S14D indicates that at least some of the ATG14L-containing complexes were capable of getting to the phagophore, possibly as a result of transient overexpression, to induce autophagy.

The ULK phosphorylation site in Beclin-1 is conserved in *C. elegans* and required for proper autophagy

To extend our observations at the organismal level and across species we used a *C. elegans* model system. During worm embryogenesis, the germline P granules (PGL granules) are selectively degraded by the autophagic machinery in somatic cells[33]. In autophagy-mutant embryos, PGL granules remain in somatic cells during early embryonic divisions owing to failed removal by autophagy[34]. To ascertain whether the conserved Ser 6 of BEC-1 (Beclin-1 worm homologue, Fig. 2c) was also required for proper autophagic induction, we generated transgenic lines with p*bec*-1::*bec*-1(WT or S6A)::*gfp* in the *bec-1(ok700)* background. In WT worms, PGL-1, a key component of PGL granules, was exclusively expressed in the two germline precursor cells (Fig. 7a, arrows mark germline cells). In contrast, *bec-1* and *unc-51* (ULK/ATG1 homologue) worms exhibited somatic cell PGL-1 staining, indicating a defect in autophagic clearance (Fig. 7a). Importantly, *bec-1*(WT) transgene expression fully rescued the defective degradation of the PGL-1 granules in the *bec-1* background (Fig. 7a). In contrast, *bec-1*(S6A) transgenic embryos contained PGL-1 body staining in the somatic cells (Fig. 7a–c). Comparable expression levels of the *bec-1* transgene were validated by western blotting (Fig. 7b). The PGL-1 staining phenotype in *bec-1*(S6A) lines varied between embryos with punctuate staining in two-thirds of embryos and diffuse staining in one-third of embryos (Fig. 7c). We also noted that the increased PGL-1 staining is less pronounced in *bec-1*(S6A) worms than in the *bec-1* worm, indicating a partial rescue of PGL body clearance by BEC-1(S6A). These data collectively demonstrate a role for both *unc-51* and the conserved Ser 6 of *bec-1* in the autophagic clearance of protein aggregates in *C. elegans* embryogenesis.

We next investigated autophagosome biogenesis in *bec-1*(WT) and *bec-1*(S6A) rescued transgenic lines. The use of anti-LGG-1 (LC3B/ATG8 homologue) antibody in worms to distinguish levels of autophagy has been established in previous studies[35]. In *bec-1* worms, the number of LGG-1 punctate structures was markedly decreased, whereas the size and intensity were increased when compared with the WT (Fig. 7d,e). This phenotype was rescued by a transgenic line containing *bec-1*(WT) but not *bec-1*(S6A) (Fig. 7d,e). Failure to rescue the autophagic defect in *bec-1*(S6A) transgenic worms is consistent with phosphorylation of Ser 6 being crucial for the initiation of autophagosome formation. Together, our data indicate that the *bec-1*(S6A) exhibits an autophagic defect largely overlapping that of *unc-51* worms, indicating that this residue is required for robust *unc-51*-dependent induction of autophagy.

DISCUSSION

Generation of PtdIns(3)P at the phagophore by VPS34 is a critical early event in autophagosome formation[36]. In yeast, PtdIns(3)P is enriched in the inner lumen of the nascent autophagosome, serving as an anchor recruiting PtdIns(3)P-binding proteins such as ATG18 (mammalian homologues are WIPI 1,2), which may play a role in the formation of the early autophagosomal membrane[37–39]. Interestingly, VPS34 activity has been reported to be repressed by amino-acid starvation, an observation at odds with our understanding of the genesis of the autophagosomal membrane[25–27]. Here we provide the mechanistic understanding for the paradoxical decrease in total cellular PtdIns(3)P with concomitant induction of PtdIns(3)P at the autophagosomal membrane on amino-acid withdrawal. VPS34 complexes devoid of pro-autophagic adaptors ATG14L and UVRAG are repressed by the removal of amino acids in an ULK-independent manner. Conversely, the activity of ATG14L-containing VPS34 complexes is strongly induced by starvation in an ULK-dependent manner that, along with changes in localization, mediates the upregulation of PtdIns(3)P at the autophagosomal membrane. Interestingly, a recent report showed that AMPK is responsible for both the activation of pro-autophagic VPS34 and repression of non-autophagic complexes on glucose starvation[24]. The ability of amino-acid withdrawal to potently inhibit total VPS34 in the absence of ULK means that the regulation of these complexes is performed by another

nutrient-sensitive pathway. Future study into the repression of total VPS34 will undoubtedly shed light on the functions of VPS34 in the starvation response.

Our study supports a model that TORC1 inhibition by amino-acid starvation leads to de-repression of ULK kinase activity. The active ULK directly phosphorylates Beclin-1 Ser 14 and activates the pro-autophagy VPS34 complexes to promote autophagy induction and maturation (Fig. 8). This model reveals a continuous signalling pathway: amino acids–TORC1–ULK1–VPS34–Beclin-1. The identified ULK1 phospho-site on Beclin-1 has no obvious conservation in yeast ATG6. It will be interesting to determine whether the link between ATG1 and ATG6 is functionally maintained in yeast; one could look at the functional conservation of TOR–ATG1 as an example. Given the complex nature of autophagy biology, the regulation of VPS34 is likely to be complex and future studies are required to have a comprehensive understanding of VPS34 regulation in response to the wide range of autophagy-inducing signals. □

METHODS

Methods and any associated references are available in the online version of the paper.

Note: Supplementary Information is available in the online version of the paper

ACKNOWLEDGEMENTS

We would like to thank H. Zhang for LGG-1 and PGL-1 antibodies; J. Jewell, C. Hansen and K. Tumaneng for critical reading of this manuscript; and M. Farquhar for electron microscopy. Phosphosite identification by mass spectrometry was performed by the Proteomics Facility at the Fred Hutchinson Cancer Research Center. Confocal analysis was performed at the UCSD Neuroscience Microscopy Shared Facility (Grant P30 NS047101). This work was supported by National Institutes of Health (NIH) grants GM51586, GM62694 and CA108941, and the Department of Defense (W81XWH-0901-0279). R.C.R. is supported by a Canadian Institutes of Health Research (CIHR) postdoctoral fellowship.

AUTHOR CONTRIBUTIONS

R.C.R. planned and performed experiments, Y.T. planned and performed experiments, H.Y., H.W.P., Y-Y.C and H.K. performed experiments, J.K., T.P.N., A.D. and K-L.G. planned experiments, R.C.R. and K-L.G. wrote the manuscript.

COMPETING FINANCIAL INTERESTS

The authors declare no competing financial interests.

Published online at www.nature.com/doifinder/10.1038/ncb2757
Reprints and permissions information is available online at www.nature.com/reprints

1. Mizushima, N. & Komatsu, M. Autophagy: renovation of cells and tissues. *Cell* **147,** 728–741 (2011).
2. Young, A. R. *et al.* Starvation and ULK1-dependent cycling of mammalian Atg9 between the TGN and endosomes. *J. Cell Sci.* **119,** 3888–3900 (2006).
3. Hara, T. *et al.* FIP200, a ULK-interacting protein, is required for autophagosome formation in mammalian cells. *J. Cell Biol.* **181,** 497–510 (2008).
4. Chan, E. Y., Longatti, A., McKnight, N. C. & Tooze, S. A. Kinase-inactivated ULK proteins inhibit autophagy via their conserved C-terminal domains using an Atg13-independent mechanism. *Mol. Cell Biol.* **29,** 157–171 (2009).
5. Backer, J. M. The regulation and function of Class III PI3Ks: novel roles for Vps34. *Biochem. J.* **410,** 1–17 (2008).
6. Yan, J. *et al.* Mouse ULK2, a novel member of the UNC-51-like protein kinases: unique features of functional domains. *Oncogene* **18,** 5850–5859 (1999).
7. Ganley, I. G. *et al.* ULK1.ATG13.FIP200 complex mediates mTOR signaling and is essential for autophagy. *J. Biol. Chem.* **284,** 12297–12305 (2009).
8. Hosokawa, N. *et al.* Nutrient-dependent mTORC1 association with the ULK1-Atg13-FIP200 complex required for autophagy. *Mol. Biol. Cell* **20,** 1981–1991 (2009).
9. Jung, C. H. *et al.* ULK–Atg13–FIP200 complexes mediate mTOR signaling to the autophagy machinery. *Mol. Biol. Cell* **20,** 1992–2003 (2009).
10. Kim, J., Kundu, M., Viollet, B. & Guan, K. L. AMPK and mTOR regulate autophagy through direct phosphorylation of Ulk1. *Nat. Cell Biol.* **13,** 132–141 (2011).
11. Egan, D. F. *et al.* Phosphorylation of ULK1 (hATG1) by AMP-activated protein kinase connects energy sensing to mitophagy. *Science* **331,** 456–461 (2011).
12. Itakura, E. & Mizushima, N. Characterization of autophagosome formation site by a hierarchical analysis of mammalian Atg proteins. *Autophagy* **6,** 764–776 (2010).
13. Volinia, S. *et al.* A human phosphatidylinositol 3-kinase complex related to the yeast Vps34p–Vps15p protein sorting system. *EMBO J.* **14,** 3339–3348 (1995).
14. Sun, Q. *et al.* Identification of Barkor as a mammalian autophagy-specific factor for Beclin 1 and class III phosphatidylinositol 3-kinase. *Proc. Natl Acad. Sci. USA* **105,** 19211–19216 (2008).
15. Itakura, E., Kishi, C., Inoue, K. & Mizushima, N. Beclin 1 forms two distinct phosphatidylinositol 3-kinase complexes with mammalian Atg14 and UVRAG. *Mol. Biol. Cell* **19,** 5360–5372 (2008).
16. Liang, C. *et al.* Autophagic and tumour suppressor activity of a novel Beclin1-binding protein UVRAG. *Nat. Cell Biol.* **8,** 688–699 (2006).
17. Takahashi, Y. *et al.* Bif-1 interacts with Beclin 1 through UVRAG and regulates autophagy and tumorigenesis. *Nat. Cell Biol.* **9,** 1142–1151 (2007).
18. Di Bartolomeo, S. *et al.* The dynamic interaction of AMBRA1 with the dynein motor complex regulates mammalian autophagy. *J. Cell Biol.* **191,** 155–168 (2010).
19. Pattingre, S. *et al.* Role of JNK1-dependent Bcl-2 phosphorylation in ceramide-induced macroautophagy. *J. Biol. Chem.* **284,** 2719–2728 (2009).
20. Zalckvar, E. *et al.* DAP-kinase-mediated phosphorylation on the BH3 domain of beclin 1 promotes dissociation of beclin 1 from Bcl-XL and induction of autophagy. *EMBO Rep.* **10,** 285–292 (2009).
21. Zhong, Y. *et al.* Distinct regulation of autophagic activity by Atg14L and Rubicon associated with Beclin 1-phosphatidylinositol-3-kinase complex. *Nat. Cell Biol.* **11,** 468–476 (2009).
22. Matsunaga, K. *et al.* Two Beclin 1-binding proteins, Atg14L and Rubicon, reciprocally regulate autophagy at different stages. *Nat. Cell Biol.* **11,** 385–396 (2009).
23. Matsunaga, K. *et al.* Autophagy requires endoplasmic reticulum targeting of the PI3-kinase complex via Atg14L. *J. Cell Biol.* **190,** 511–521 (2010).
24. Kim, J. *et al.* Differential regulation of distinct Vps34 complexes by AMPK in nutrient stress and autophagy. *Cell* **152,** 290–303 (2013).
25. Byfield, M. P., Murray, J. T. & Backer, J. M. hVps34 is a nutrient-regulated lipid kinase required for activation of p70 S6 kinase. *J. Biol. Chem.* **280,** 33076–33082 (2005).
26. Gulati, P. *et al.* Amino acids activate mTOR complex 1 via Ca^{2+}/CaM signaling to hVps34. *Cell Metab.* **7,** 456–465 (2008).
27. Nobukuni, T. *et al.* Amino acids mediate mTOR/raptor signaling through activation of class 3 phosphatidylinositol 3OH-kinase. *Proc. Natl Acad. Sci. USA* **102,** 14238–14243 (2005).
28. Wei, Y., Pattingre, S., Sinha, S., Bassik, M. & Levine, B. JNK1-mediated phosphorylation of Bcl-2 regulates starvation-induced autophagy. *Mol. Cell* **30,** 678–688 (2008).
29. Lee, E. J. & Tournier, C. The requirement of uncoordinated 51-like kinase 1 (ULK1) and ULK2 in the regulation of autophagy. *Autophagy* **7,** 689–695 (2011).
30. Gillooly, D. J. *et al.* Localization of phosphatidylinositol 3-phosphate in yeast and mammalian cells. *EMBO J.* **19,** 4577–4588 (2000).
31. Bach, M., Larance, M., James, D.E. & Ramm, G. The serine/threonine kinase ULK1 is a target of multiple phosphorylation events. *Biochem. J.* **440,** 283–291 (2011).
32. Fan, W., Nassiri, A. & Zhong, Q. Autophagosome targeting and membrane curvature sensing by Barkor/Atg14(L). *Proc. Natl Acad. Sci. USA* **108,** 7769–7774 (2011).
33. Zhang, Y. *et al.* SEPA-1 mediates the specific recognition and degradation of P granule components by autophagy in *C. elegans*. *Cell* **136,** 308–321 (2009).
34. Zhao, Y., Tian, E. & Zhang, H. Selective autophagic degradation of maternally-loaded germline P granule components in somatic cells during *C. elegans* embryogenesis. *Autophagy* **5,** 717–719 (2009).
35. Tian, Y. *et al. C. elegans* screen identifies autophagy genes specific to multicellular organisms. *Cell* **141,** 1042–1055 (2010).
36. Petiot, A., Ogier-Denis, E., Blommaart, E. F., Meijer, A. J. & Codogno, P. Distinct classes of phosphatidylinositol 3′-kinases are involved in signaling pathways that control macroautophagy in HT-29 cells. *J. Biol. Chem.* **275,** 992–998 (2000).
37. Obara, K. & Ohsumi, Y. PtdIns 3-kinase orchestrates autophagosome formation in yeast. *J. Lipids* **2011,** 498768 (2011).
38. Suzuki, K., Kubota, Y., Sekito, T. & Ohsumi, Y. Hierarchy of Atg proteins in pre-autophagosomal structure organization.. *Genes Cells* **12,** 209–218 (2007).
39. Obara, K., Noda, T., Niimi, K. & Ohsumi, Y. Transport of phosphatidylinositol 3-phosphate into the vacuole via autophagic membranes in *Saccharomyces cerevisiae*. *Genes Cells* **13,** 537–547 (2008).

METHODS

Antibodies. Anti-phospho-Beclin-1(Ser 14) was obtained from Abbiotec (Cat#254515). Anti-LC3B (Cat#2775 for western blotting (WB)), VPS34 (Cat#4263 for WB), Beclin-1 (Cat#3738 for WB), ULK1 (Cat#8054), pULK1 Ser 757 (Cat#6888) and phospho-S6K (Cat#9205) were purchased from Cell Signaling Technology. Anti-Atg14L (Cat#PD026 for immunoprecipitation), UVRAG (Cat#M160-3) and LC3B (Cat#PM036 for immunostaining) antibodies were obtained from MBL. Immunoprecipitation was performed using Anti-VPS34 (Echelon, Cat#ZR015) and Beclin-1 (Bethyl Cat#A302-567A) antibodies. Anti-vinculin (Cat#V9264), alpha-tubulin (Cat#T6199), Flag (Cat#F3165) and Atg14L (Cat#A6358) antibodies were obtained from Sigma and used for western blotting. Anti-HA (Clone 16B12, Cat#MMS-101P) and Myc (Clone 9E10, Cat#MMS-150P) antibodies were obtained from Covance. Anti-actin (Cat# Ab3280) antibody was obtained from Abcam.

Cell culture. Immortalized MEFs were cultured in high-glucose DMEM supplemented with 10% FBS (Hyclone), 50 μg ml^{-1} penicillin/streptromycin, 1 mM sodium pyruvate, 55 μm 2-mercaptoethanol and 0.1 mM non-essential amino acids (each obtained from Invitrogen). Amino-acid-free medium was made according to Gibco standard recipe omitting all amino acids and supplemented as above without addition of non-essential amino acids and substitution with dialysed FBS (Invitrogen). HEK293 cells were grown in similar media omitting the 2-mercaptoethanol. Medium was replenished the night before starvation experiments and again three hours before withdrawal of amino acids or addition of mTOR inhibitors. *FIP200*$^{-/-}$ MEFs were a gift from J-L. Guan, University of Michigan (USA). *ULK1*$^{-/-}$ ULK2 knockdown MEFs were generated as previously described[10]. The ATG14L–FLAG–6His-inducible U2OS cell line was a gift from Q. Zhong, University of California Berkeley (USA).

Generation of knockdown reconstitution lines. HeLa cells were stably infected with shRNA against Beclin-1 (target 5′-CTCAGGAGAGGAGCCATTTAT-3′) or scrambled control in the pLKO.1 lentiviral background. Lentiviral particles were made by cotransfection with psPAX2 and pMD2.G plasmids into HEK293T cells. Viral supernatants were collected from 48 to 60 h. Cleared supernatant was filtered through a 0.45 μm filter and applied every 12 h on target cells for 3 rounds. Polybrene (4 μg ml^{-1}; Sigma) was supplemented to viral supernatants. Twenty-four hours after final infection, stable shRNA-containing populations were obtained by selection with 2 μg ml^{-1} puromycin (Invivogen). Beclin-1 shRNA HeLa cells were then infected with retroviral particles expressing shRNA-resistant HA–Beclin-1(WT or mutant) in the pQCXIH background. Retroviral particles were generated by transfection of HA–Beclin-1 constructs into Phoenix packaging cell lines. Following the same infection protocol described for lentiviral particles. Secondary selection was performed with 1 μg ml^{-1} puromycin and 250 μg ml^{-1} hygromycin (Invitrogen). Polyclonal populations were screened until WT and mutant lines were generated that had near endogenous Beclin-1 reconstitution levels.

Western blotting and immunoprecipitation. Whole-cell extracts were generated by direct lysis with 1× denaturing Laemmli sample buffer. Samples were boiled for 10 min at 100 °C and resolved by SDS–PAGE. Immune complexes were obtained from cells lysed in mild lysis buffer (10 mM Tris at pH 7.5, 2 mM EDTA, 100 mM NaCl, 1% NP-40, 50 mM NaF, supplemented at time of lysis with 1 mM Na_3VO_4 and protease inhibitor cocktail–EDTA (Roche)). Antibodies were prebound to protein A beads (Repligen) overnight in MLB with 1% BSA. Beads were washed 1× with MLB and mixed with cleared cell lysates for 2 h followed by 5 washes with MLB. Beads were boiled in 1× denaturing Laemmli sample buffer for 5 min before resolving by SDS–PAGE.

Quantification of western blot. Statistical analysis was performed on biological repeats using ImageJ and application of Student's two-tailed *t*-test. Error bars represent the standard deviation in normalized fold changes in observed induction or repression.

Mass spectrometry. A gel band corresponding to the Beclin-1 GST fusion protein was cut from a SDS–PAGE gel after an *in vitro* kinase reaction. The gel band was subjected to in-gel trypsin digestion and the resulting peptide mixture was subjected to liquid chromatography coupled to tandem mass spectrometry. Protein and modification identification was performed with the database search algorithm X!Tandem and peptide identifications were validated with Peptide Prophet.

Indirect immunofluorescence microscopy. Fibronectin-coated coverslips were placed in 24-well plates and cells were seeded the night before starvation or treatment. Cells were fixed by 4% paraformaldehyde in PBS for 15 min, followed by permeabilization with 50 μg ml^{-1} digitonin in 2% BSA, and 2% goat serum in PBS for 10 min. Cells were blocked in 2% BSA, and 2% goat serum in PBS for 30 min and then incubated with primary antibodies in the same buffer for 1 h at room temperature. The biotin–2XFYVE domain probe was incubated separately from other primary antibodies to reduce background. Slides were washed 3× in PBS followed by incubation of secondary antibody in 2% BSA, and 2% goat serum in PBS for 1 h at room temperature. Slides were washed 3× in PBS and mounted. Images were captured with an Olympus FV1000 confocal microscope.

Quantification of indirect immunofluorescence signal. Confocal microscopy images were used to determine co-localization using an automated protocol built in the Velocity 3D imaging software to reduce bias. The same protocol was applied to each field of view and across samples. Quantification was performed on representative experiments with an average of 7 unique fields of view. For *C. elegans* experiments each embryo was scored as $n = 1$, in a representative experiment. Puncta and staining patterns of embryos were quantified using a blind manual scoring method.

Electron microscopy. HeLa lines were fixed in modified Karnovsky's fixative (1.5% glutaraldehyde, 3% paraformaldehyde and 5% sucrose in 0.1 M cacodylate buffer, at pH 7.4) for 15 min at room temperature followed by overnight at 4 °C. The following day they were treated with 1% osmium tetroxide and 0.1 M cacodylate buffer for 1 h. Samples were stained in 1% uranyl acetate and dehydrated with ethanol. Epoxy-resin-embedded samples were sectioned (60–70 nm), and placed on Formvar, carbon-coated copper grids. Grids were stained with uranyl acetate and lead nitrate. Images were obtained using a JEOL 1200EX II transmission electron microscope and photographed on a Gatan digital camera.

Statistical analysis. Error bars for microscopy (with the exception of *C. elegans* data) were presented as the standard deviation between unique fields of view within a representative experiment. In *C. elegans* microscopy the error bars represent the standard deviation between unique embryos. Error bars for western blot analysis represent the standard deviation between densitometry data collected from 3 or more unique biological experiments. Statistical significance was determined using unpaired Student's two-tailed *t*-test for two data sets.

***In vitro* ULK1 kinase assay.** ULK1 proteins were immunoprecipitated and extensively washed with MLB (once) and RIPA buffer (50 mM Tris at pH 7.5, 150 mM NaCl, 50 mM NaF, 1 mM EDTA, 1 mM EGTA, 0.05% SDS, 1% Triton X-100 and 0.5% deoxycholate) once, followed by washing with MLB buffer once followed by equilibration with ULK1 assay buffer (KBB supplemented with 0.05 mM dithiothreitol 10 μM cold ATP) and 2 μCi γ-^{32}P[ATP] per reaction. Reaction was quenched by direct addition of 4× Laemmli buffer followed by boiling for 5 min and resolution by SDS–PAGE. The analysis of some kinase reactions necessitated the separation of the kinase and substrate. In these cases one of the components (either kinase or substrate) was left on beads and the eluant and washed beads were loaded on separate gels. Substrate and kinase were separated in kinase assays shown in Fig. 2a,b,d. Fractions of the total kinase reaction are shown in Supplementary Fig. S2a,d. All *in vitro* kinase reactions that were analysed by western blotting with the phospho-Beclin-1 antibody were fractions from the total reaction.

***In vitro* VPS34 lipid kinase assay.** Immuno-purified complexes were equilibrated in 1× kinase base buffer (20 mM HEPES at pH 7.4, 1 mM EGTA, 0.4 mM EDTA and 5 mM $MgCl_2$). One half volume was taken for input; the remainder was centrifuged and excess 1× KBB was removed. Forty microlitres of 1× kinase assay buffer was added to the beads (1× KBB supplemented with 0.1 mg ml^{-1} phosphatidylinositol, 50 μM cold ATP, 5 μCi γ-^{32}P[ATP], 5 mM $MnCl_2$ and 50 μM dithiothreitol) followed by incubation at 37 °C for 30 min with vigorous shaking. Reaction was quenched by direct addition of 10 μl 1 M HCl, followed by lipid extraction with 2 volumes of methanol/$CHCl_3$ (1:1). Samples were vortexed for 1 min and centrifuged at maximum *g* for 2 min. The aqueous phase was discarded and the organic phase was loaded on a thin-layer chromatography plate (Whatman). Resolution of phospho-lipid was achieved using a buffer composition of CHCl/methanol(99%)/NH_4OH(30%)/water (129:100:4.29:24). Resolved plates were analysed by autoradiography.

Mutagenesis. Site-directed mutagenesis was performed following Stratagene Quikchange kit instructions,with the following modifications: primer lengths designed to the manufacturer's specifications were generally reduced by 4 nucleotides 4 nucleotides on each end; primers were purified using standard desalt quality; template amount was increased to 50 ng; cycles were increased to 25; specificity of mutagenesis was confirmed by direct sequencing.

Protein purification. For bacterial GST-fusion proteins, Beclin-1 (including truncations and mutations) were cloned into the pGEX-KG vector and transformed into BL21 *E. coli*. Depending on protein stability, induction was either performed on cultures ($D_{600\,nm} = 0.5$–0.8) at 16 °C overnight with 0.5 mM IPTG or at 37 °C

DOI: 10.1038/ncb2757

for 2 h. Bacteria were pelleted and resuspended in PBST (PBS, 0.5% Triton X-100, phenylmethyl sulphonyl fluoride and 2 mM b-mercaptoethanol) and lysed by ultrasonication at 4 °C. Cleared lysates were subjected to glutathione Sepharose. Beads were washed with PBST and bound proteins were eluted using reduced glutathione according to the manufacturer's instructions. Eluants were dialysed against 20 mM Tris–HCl at pH 8.0 with 10% glycerol.

To generate immunoprecipitated ULK1 kinase, 3 × HA–ULK1 was transfected into HEK293 cells and immunoprecipitated with anti-HA antibody. Immunoprecipitated HA–ULK1 was washed as described in the kinase section of the methods. To generate liquid ULK1 kinase, FLAG–ULK1 was transfected into HEK293 cells and immunoprecipitated using anti-DYKDDDDK antibody (Agilent Technologies #200474). Immune-complexes were washed as described above and eluted in 4 bead volumes of PBS, 400 μg ml^{-1} and 3 × FLAG peptide for 30 min. Eluant was dialysed (50 kDa molecular weight cutoff) for 3 h in 1× kinase assay buffer, 10%glycerol. Active GST–ULK1 (1–649) and GST–ULK2 (1–478) from insect cells was purchased from CQuential Solutions.

***C. elegans* strains.** The following strains were used in this work: *unc-51(e1189)* and *VC424 bec-1* (ok700)/nTl (*qIs51*). *ok700* is an allele that has a 1,377-base-pair deletion and is considered equivalent to a null allele of *bec-1*. Homozygous *bec-1(ok700)* is lethal so *bec-1(ok700/+)* worms were used to generate transgenic lines. Bristol N2 line was used for the wild-type strain.

***C. elegans* reporter construction.** Both *bec-1* genomic DNA and *bec-1* complementary DNA driven by bec-1 endogenous promoter were cloned into the pPD95.79 vector. The mutant S6A was made based on the WT constructs. The constructs were co-injected with pRF4(*rol-6(su1006)*) into VC424 worms and two stable transgenic lines were analysed for each reporter.

***C. elegans* immunofluorescence.** Embryos were obtained from well-fed adult hermaphrodites of transgenic lines by the freeze-cracking method. The slides were fixed, blocked and incubated with diluted antibodies at 4 °C overnight. The worms were then washed three times with PBST (0.5%) and incubated with rhodamine-conjugated secondary antibody. Slides were viewed using an Epitome microscope.

Bec-1 has a maternal effect that rescues the autophagy defect in the *bec-1*-null embryos arising from *bec-1(-/+)* worms. Therefore, *bec-1*-null embryos shown are from the *bec-1*-null/pBEC-1::BEC-1::GFP non-integrated transgenic lines, by selecting embryos that do not express the GFP transgene. Both anti-PGL-1 and anti-LGG-1 antibodies were gifts from H. Zhang's laboratory in NIBS (China).